Full Paper

Propellants, Explosives, Pyrotechnics

DOI: 10.1002/prep.201900402

Salts of Picramic Acid – Nearly Forgotten Temperature-Resistant Energetic Materials

Maximilian H. H. Wurzenberger,[a] Jasmin T. Lechner,[a] Marcus Lommel,[a] Thomas M. Klapötke,[a] and Jörg Stierstorfer*[a]

Dedicated to Dr. Klaus Römer on the Occasion of his 80th Birthday

Abstract: Thermally stable explosives are becoming more and more important nowadays due to their important role in the oil and mining industry. The requirements of these explosives are constantly changing. Picramate-based compounds are poorly investigated towards their energetic properties as well as sensitivities. In this work, 13 different salts of picramic acid were synthesized as potential energetic materials with high thermal stability in a simple one-step reaction and compared with commercially used lead picramate. The obtained compounds were extensively characterized by e.g. XRD, IR, EA, DTA, and TGA. In addition, the sensitivities towards impact and friction were determined with the BAM drop hammer and the BAM friction tester. Also, the electrostatic discharge sensitivity was explored. Calculations of the energetic performance of selected compounds were carried out with the current version of EXPLO5 code. Therefore, heats of formation were computed and X-ray densities were converted to room temperature. Some of the synthesized salts show promising characteristics with high exothermic decomposition temperatures. Especially, the water-free rubidium, cesium, and barium salts **5**, **6** and **10** with decomposition temperatures of almost 300 °C could be promising candidates for future applications.

Keywords: Picramic Acid · Energetic Materials · Energetic Salts · Thermally Stable Explosives · Nitroaromatic Compounds

1 Introduction

The field of energetic materials is manifold and can be divided into several subgroups, such as propellants, primary or high explosives, which is leading to numerous and diverse applications [1–3]. Especially, due to the increased environmental awareness, there are many research groups around the world working on the development of ever more efficient molecules. The new compounds should, if possible, be less toxic and harmful to the environment than current molecules and at the same time also cheaper to produce [4–6]. Various strategies exist for designing new energetic materials, like increasing the energy of a molecule by ring or cage strain. Another approach is the synthesis of nitrogen-rich compounds, which release a lot of energy during their decomposition, due to their large endothermic heat of formation. The third strategy is the combination of fuel (carbon-backbone) and oxidizer (nitro groups) in one molecule. Various examples for this concept are displayed in Chart 1, with 2,4,6-trinitrotoluene (TNT) being the most favorite one, since it was the most commonly used explosive in World War I and is still used in explosive charges today [2, 7].

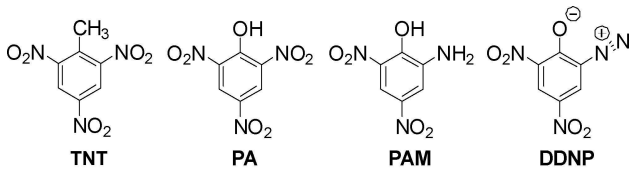

Chart 1. Chemical structures of 2,4,6-trinitrotoluene (TNT), 2,4,6-trinitrophenol (PA), 2-amino-4,6-dinitrophenol (PAM), and diazodinitrophenol (DDNP).

Another famous representative of this group is picric acid (PA), which replaced black powder at the end of the 19th century in military applications [8]. Later it was substituted by TNT itself because it caused undesired formations of very sensitive

[a] *M. H. H. Wurzenberger, J. T. Lechner, M. Lommel, T. M. Klapötke, J. Stierstorfer*
Department of Chemistry
Ludwig-Maximilian University of Munich
Butenandtstr. 5–13, 81377 Munich (Germany)
**e-mail: jstch@cup.uni-muenchen.de*
Homepage: http://www.hedm.cup.uni-muenchen.de

Supporting information for this article is available on the WWW under https://doi.org/10.1002/prep.201900402

metal salts in grenades and mines [2, 9]. A rather uncommon representative is 2-amino-4,6-dinitrophenol, also known as picramic acid (PAM), which can be obtained by partial reduction of PA with sodium hydrogen sulfide, ammonium sulfide or hydrazine. PAM is known for its explosive character but the neutral compound and the associated sodium salt are more familiar as ingredients for 'henné' color in hair and skin colorants [10–12]. Indeed, picramic acid and some of its soluble salts are more well-known as precursors for the synthesis of diazodinitrophenol (DDNP), an efficient heavy metal-free primary explosive [10, 13].

In 1961 Glowiak *et al*. demonstrated, based on lead picrate and lead picramate, that the replacement of a nitro group by an amino group leads to an increase in thermal stability with simultaneously reduced impact sensitivity [14]. This was also confirmed by J. P. Agrawal, who developed some approaches to increase the thermal stability of energetic molecules. He particularly emphasized the concepts 'salt formation' and 'introduction of amino groups' [1]. Agrawal *et al.* examined the energetic characteristics of iron(II), cobalt(II), nickel(II), copper(II), silver(I), zinc(II), cadmium(II), and mercury(I) picramate [15–17]. A few years later, Srivastava and Agrawal investigated titanium(IV), zirconium(IV) and thorium(IV) as well as palladium(IV) and uranium(IV) picramate [18, 19]. All metal picramates showed energetic properties but are only partly investigated, except lead picramate, which is the only salt used for industrial applications nowadays, especially in fuse head compositions of electric detonators [20, 21].

Accordingly, alkali and alkaline earth picramates, as well as ammonium picramate, could be promising thermally stable energetic compounds. In this work, these compounds were synthesized as well as their energetic properties studied and compared. A few already known salts were re-investigated in detail, due to the lack of analytical data in literature.

2 Experimental Section

Caution! *All investigated compounds are energetic materials and some of them show increased sensitivities towards various stimuli (e.g. elevated temperatures, impact, friction or electronic discharge). Although no hazards occurred, proper security precautions (safety glasses, face shield, earthed equipment and shoes, leather jacket, Kevlar sleeves, and earplugs) have to be worn while synthesizing and handling the described compounds.*

More information on the general methods and syntheses of compounds **2–15** can be found in the Supporting Information.

3 Results and Discussion

3.1 Synthesis

Sodium picramate monohydrate (**1**) was available in sufficient quantities in the research group and can be synthesized according to a literature procedure (Scheme 1) [22]. It was used as starting material to prepare picramic acid (**2**) (Scheme 2) by straightforward protonation with hydrochloric acid.

The isolated picramic acid (**2**) was further reacted in simple metathesis reactions to the corresponding salts **3–14**. It was dissolved in ethanol and a metal salt of the desired cation in water was added (Scheme 2), which led in all cases to a darkening of the solution. For a successful synthesis, an alkaline milieu had to be ensured during the whole reaction. For obtaining the alkali salts of picramic acid, the corresponding carbonates were used. Compounds **3–6** were filtered off after crystallization of sufficient amounts during evaporation of the solvent in air. For the syntheses of the alkaline earth salts **7–10** the corresponding metal hydroxides were used. Magnesium picramate (**7**) was obtained as pentahydrate in the form of single crystals suitable for X-ray diffraction experiments. The remaining alkaline earth salts could only be isolated as microcrystalline solids, due to their low solubility. For the synthesis of zinc(II) picramate (**11**), basic zinc(II) carbonate was used. The low solubility of $Zn(PAM)_2$ leads to the immediate precipitation of the product after mixing of the solutions. Similar circumstances were observed during the synthesis of silver(I) and copper(II) picramates (**12** and **13**), starting from the corresponding nitrate salts. Single crystals of **11** and **12** were obtained by layering aqueous solution of the nitrate salts with ethanolic solutions of HPAM to ensure slow formation at the phase boundary.

The yields can be increased by evaporation of the remaining mother liquor.

Ammonium picramate (**14**) was received by the addition of aqueous ammonia to the solution of picramic acid. After evaporation of the solvent, **14** was obtained as crystalline material. In case of lead picramate (**15**), the reaction of the free acid with a soluble lead salt did not lead to the formation of the desired product. Instead, sodium picramate

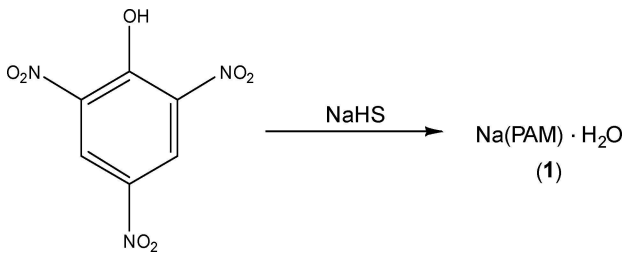

Scheme 1. Synthesis of sodium picramate (**1**, Na(PAM)).

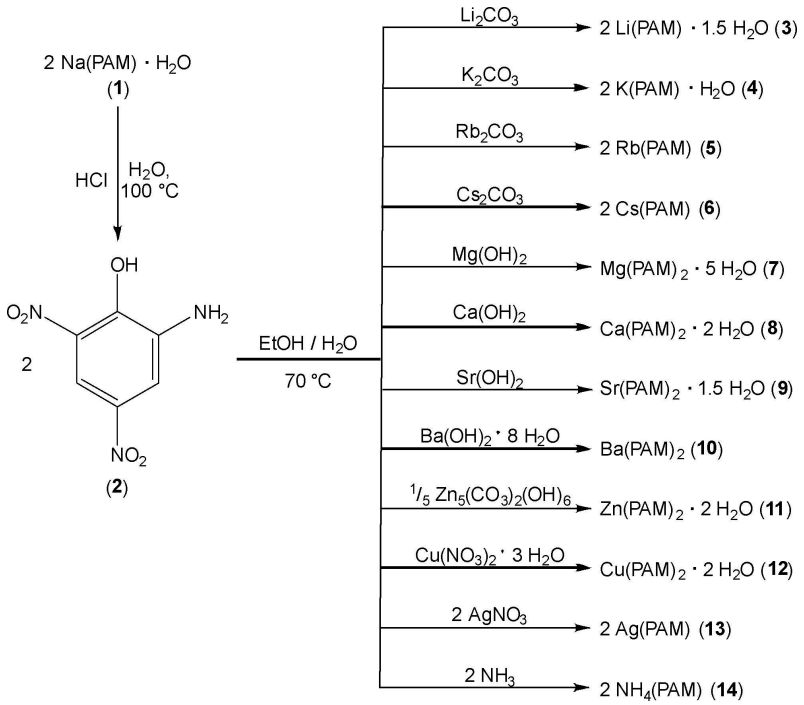

Scheme 2. Reaction scheme for the synthesis of the energetic salts **3–14**.

(**1**) was utilized as starting material (Scheme 3) leading to the direct precipitation of lead picramate.

3.2 Crystal Structures

Until today only the crystal structures of the free acid, as well as the potassium salt, were measured at room-temperature and published as private communications [23,24]. Therefore, low-temperature single-crystal X-ray diffraction experiments of compounds **1–7**, **10 b**, **11**, **12**, and **14** were performed. The crystal structures have been uploaded to the CSD database and are available under the CCDC numbers 1965957 (**1**), 1965965 (**2**), 1965964 (**3**), 1965963 (**4**), 1965958 (**5**), 1965966 (**6**), 1965967 (**7**), 1965960 (**10 b**), 1965962 (**11**), 1965959 (**12**), and 1965961 (**14**). Due to the very low solubility of pure barium picramate (**10**), it was only possible to obtain single crystals from saturated DMSO solutions. This led to the incorporation of both, DMSO and water solvent molecules (**10 b**). Details on the measurement

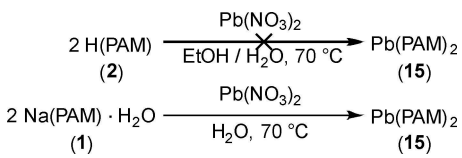

Scheme 3. Reaction scheme for the preparation of lead picramate (**15**).

and refinement data of all structures are given in the SI (Table S1–3).

The neutral compound **2** crystallizes in the form of red blocks in the triclinic space group *P*-1 with a density of 1.730 g cm^{-3} (123 K) and four molecules per unit cell. The bond lengths are in the typical range of comparable compounds and all non-hydrogen atoms, except the oxygens of the nitro groups, are within one plane (Figure 1). Latter ones are only slightly twisted out of the benzol layer.

Compared to the parent compound **2**, the deprotonation and interaction with the cations in all other compounds are leading to a shortening of the C–O and elongation of the C–N bonds of the amino groups. The only exception is cesium salt **6** with a contraction of both bonds. The nitro groups in all structures show bonds with almost the same lengths and only vary in the level of twisting out of the benzol plane.

Except of **3** (*P*-1), all alkali salts are crystallizing in monoclinic space groups (**1**: *Pc*; **4**/**5**: $P2_1/c$; **6**: *C*2/*c*) with increasing densities (Li: 1.707 g cm^{-3} (121 K) < Na: 1.791 g cm^{-3} (127 K) < K: 1.837 g cm^{-3} (135 K) < Rb: 2.226 g cm^{-3} (122 K) < Cs: 2.526 g cm^{-3} (135 K)) in terms of atomic number. A similar trend can be observed in terms of the coordination sphere around the cations: Li: CN = 4/5, Na: CN = 6, K: CN = 9, Rb: CN = 9, Cs: CN = 12. This is also influencing the polymeric structures. While lithium compound **3** is building up dimers consisting of two asymmetric units, sodium, (**1**) as well as potassium (**4**) picramate, are forming 2D polymeric layers and the rubidium (**5**), as well as cesium (**6**) salt, consist as 3D networks.

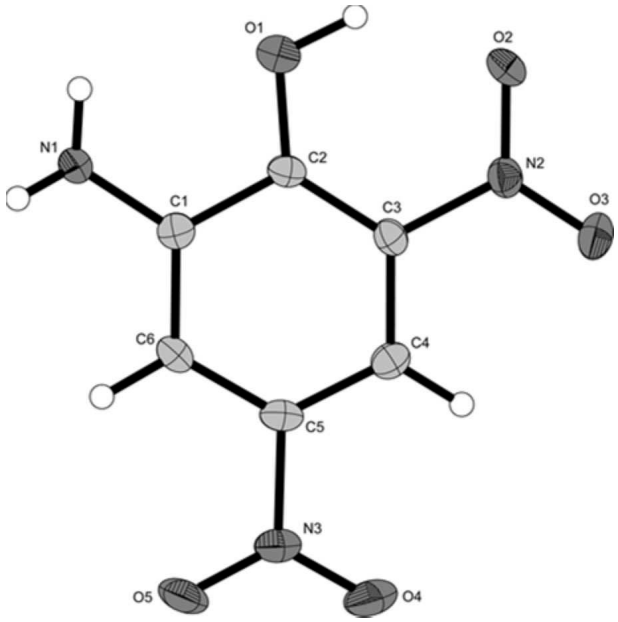

Figure 1. Molecular structure of **2**. Thermal ellipsoids of non-hydrogen atoms in all structures are set to the 50% probability level. Selected bond lengths (pm): C1–N1 135.5(2), C2–O1, 133.1(2), C3–N2 145.3(2), N2–O2 124.4(2), N2–O3 122.0(2), C5–N3 146.4(2), N3–O4 122.5(2), N3–O5 122.4(2), C1–C2 141.9(2), C2–C3 139.9(2), C3–C4 139.5(2), C4–C5 137.6(3), C5–C6 139.5(2), C6–C1 139.4(2).

The dimeric structure of **3** consists of two asymmetric units containing two different lithium ions (Figure 2). While Li1 shows a rather uncommon fivefold coordination by two chelating PAM anions and one additional aqua ligand, Li2 is tetrahedrally coordinated by one amino and one nitro group as well as two water molecules. Furthermore, the two inner anions each are bridging between three cations and the outer two are only coordinating to one lithium ion.

Similar to compound **3**, which crystallizes as sesquihydrate, sodium (**1**) and potassium (**4**) picramate are also present as mono- and sesquihydrate, respectively (Figure 3).

The only water-free alkaline salts are Rb(PAM) (**5**) and Cs(PAM) (**6**) (Figure 4). Magnesium picramate (**7**) crystallizes as pentahydrate in the form of brown rods in the monoclinic space group $P2_1/c$ with a density of 1.735 g cm^{-3} (109 K) and two molecules per unit cell. There are two different coordinated magnesium cations present, which are both octahedrally coordinated. Mg1 is chelated by two PAM anions and two monodentate aqua ligands, whereas Mg2 is solely bounded by aqua ligands. The unit cell is completed with two non-coordinating water molecules and picramate anions with a significantly twisted nitro group (Figure 5).

Recrystallization of water-insoluble $Ba(PAM)_2$ (**10**) from DMSO gave single crystals of **10 b** and leads to the incorporation of water as well as solvent molecules. It crystallizes in the form of red rods in the monoclinic space group $P2_1/n$ and a density of 1.949 g cm^{-3} (127 K). The barium cation is elevenfold coordinated by two anions and one aqua as well as DMSO ligand. The molecular unit is completed by one crystal water molecule (Figure 6).

The zinc(II) (**11**) and copper(II) (**12**) salts of picramic acid crystallize isotypically in the triclinic space group *P*-1 with similar cell axes and volume as well as comparable densities. Both compounds show an octahedral coordination sphere around the central metal, whereas the two aqua ligands occupy the axial positions and two chelating anions are in equatorial positions (Figure 7). Furthermore, a typical Jahn-Teller distortion can be observed along the O6–Cu1–O6^{i} axis.

Ammonium picramate (**14**) crystallizes as anhydrous salt in the form of orange platelets in the monoclinic space group $P2_1/c$ with four molecules per unit cell (Figure 8). It possesses the lowest density (1.693 g cm^{-3}@104 K) of all compounds.

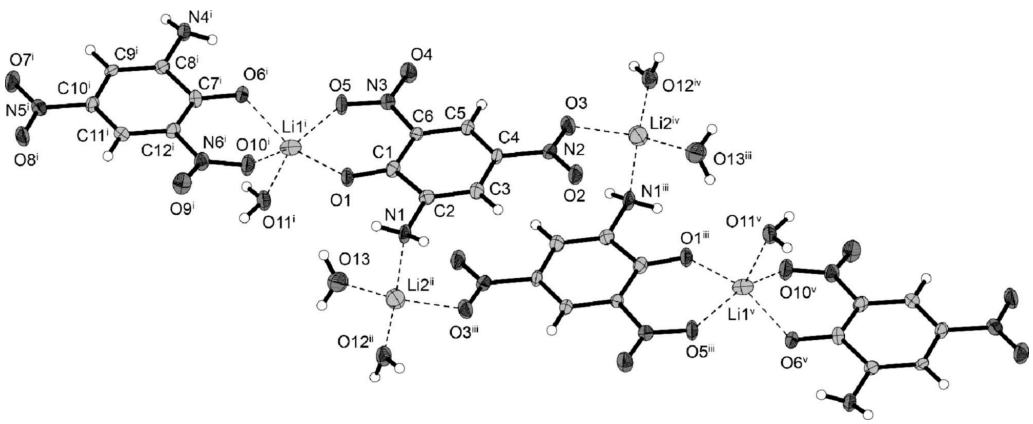

Figure 2. Dimeric structure of **3**. Selected bond lengths (pm): Li1^{i}–O1 190.4(8), Li1^{i}–O5 205.0(8), Li1^{i}–O6^{i} 196.5(8), Li1^{i}–O10^{i} 206.2(8), Li1^{i}–O11^{i} 202.7(9), Li2^{ii}–O3^{iii} 201.8(8), Li2^{ii} –O12^{ii} 184.8(9), Li2^{ii} –O13 190.3(9). Symmetry codes: i) 1−x, 1−y, −z; ii) x, −1+y; iii) −x, −y, 1−z; iv) −x, 1−y, 1−z; v) −1+x, −1+y, 1+z.

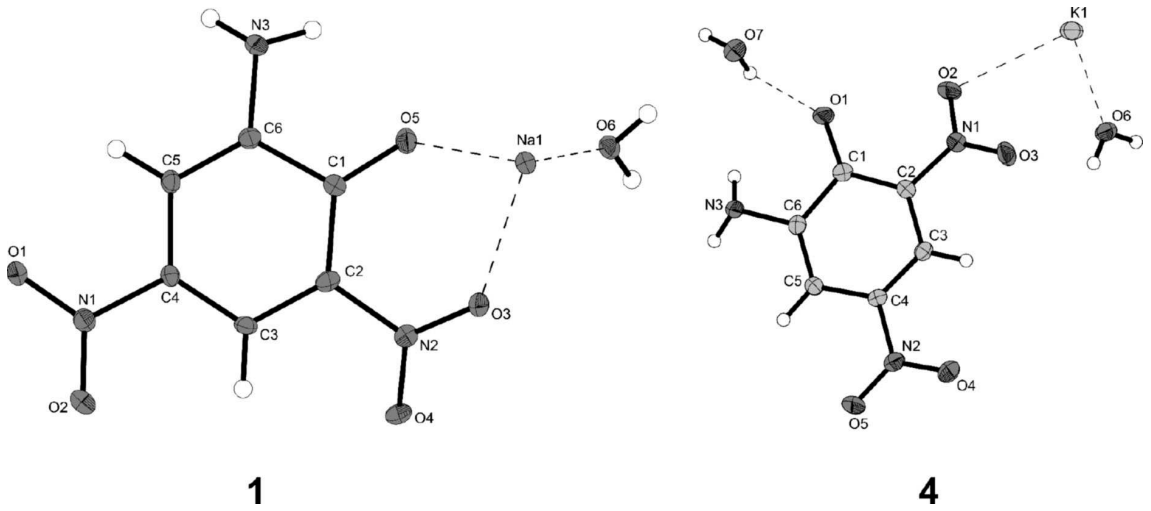

Figure 3. Molecular structure of **1** (left) and extended molecular structure of **4** (right). Selected bond lengths (pm) of **1**: Na1—O3 245.0(6), Na1—O5 232.5(6), Na1—O6 235.9(7). Selected bond lengths (pm) of **4**: K1—O2 281.33(15), K1—O3 295.71(16) K1—O6 273.64(16).

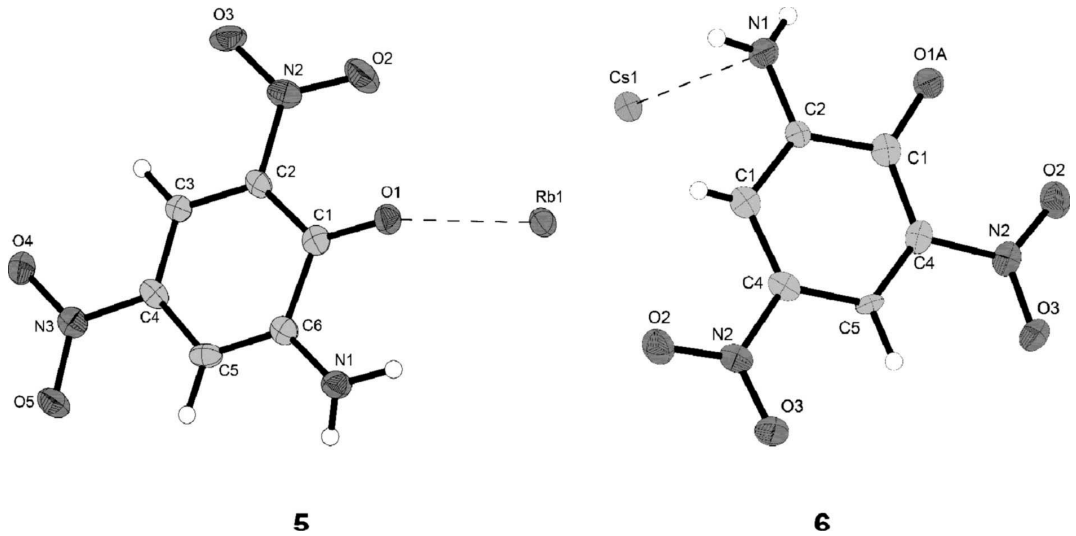

Figure 4. Molecular structure of **5** (left) and **6** (left). Selected bond length (pm) of **5**: Rb1—O1 280.3(3). Selected bond length (pm) of **6**: Cs1—N1 343.47(9).

3.3 Physiochemical Properties

The physicochemical properties of all compounds, except **10b**, were investigated and therefore thermal stability measurements were performed as well as their sensitivities towards external stimuli were determined. Furthermore, calculations of the heat of formations of **2** and **14** were made using the EXPLO5 code.

Potassium picramate (**4**), which crystallizes as sesquihydrate, seems to lose half a crystal water molecule when stored at ambient conditions. Elemental analysis as well as thermogravimetric analyses only show the presence of one molecule of water.

3.3.1 Thermal Analysis

The exothermic decomposition temperatures determined via differential thermal analysis (DTA) are listed in Table 1 together with the obtained sensitivity values. The DTA measurements were performed with a linear heating rate of $\beta = 5\,^{\circ}C\,min^{-1}$ from 30 °C to 400 °C and critical events are given as onset temperatures. The plots of the measurements can be seen in Figure 9 and S5–7. Both sodium salt **1** and picramic acid (**2**) show an endothermic event at 174 and 175 °C, respectively. Whereas **1** first loses its crystal water and decomposes afterwards at 292 °C, the neutral compound **2** melts shortly before it shows an exothermic decomposition at 217 °C. In general, it can be seen that all

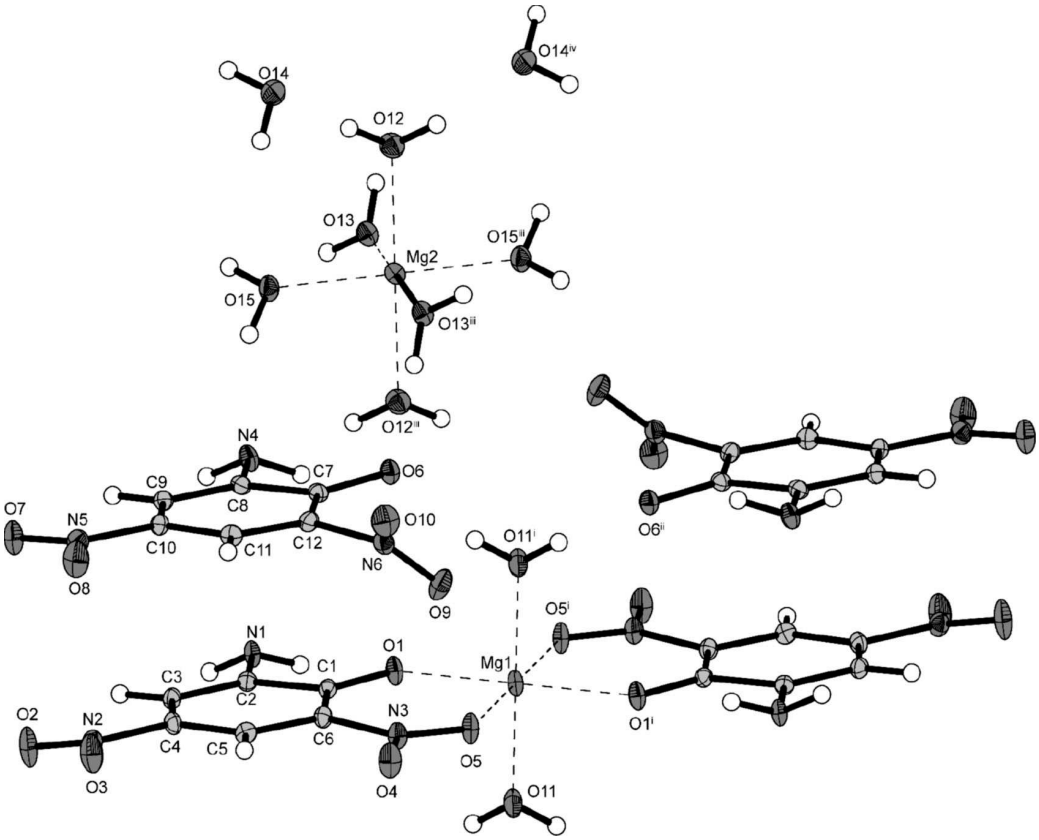

Figure 5. Molecular structure of **7**. Selected bond lengths (pm): Mg1–O1 197.29(13), Mg1–O5 210.23(13), Mg1–O11 202.39(15), Mg2–O12 205.88(14), Mg2–O13 207.10(14), Mg2–O15 205.93(13). Symmetry codes: i) 2−x, −y, −z; ii) 1−x, −y, −z; iii) 1−x, −y, 1−z; iv) −x, −y, −z.

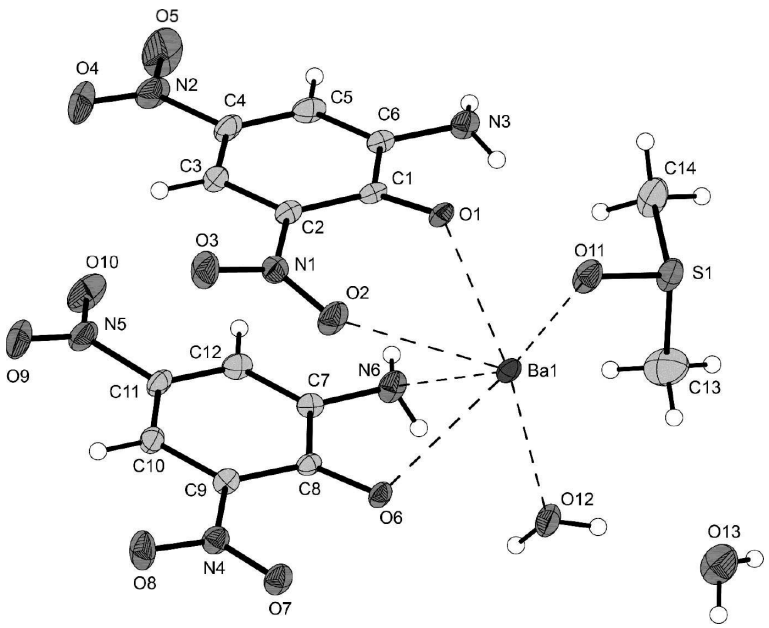

Figure 6. Molecular structure of **10b**. Selected bond lengths (pm): Ba1–O1 267.4(2), Ba1–O2 308.0(2), Ba1–O6 283.3(2), Ba1–O11 268.7(2), Ba1–O12 280.0(3), Ba1–N6 305.1(3).

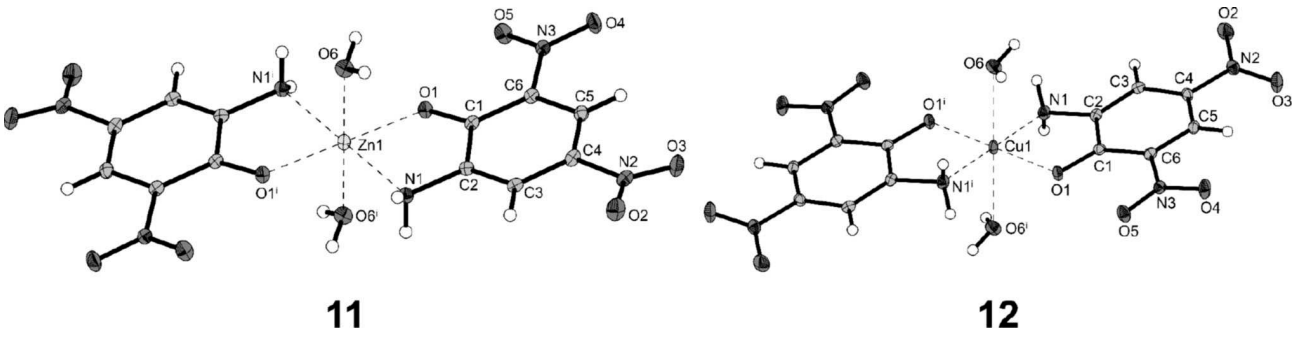

Figure 7. Molecular structures of **11** (left) and **12** (right). Selected bond lengths (pm) of **11**: Zn1–O1 207.15(16), Zn1–O6 218.70(18), Zn1–N1 211.7(2). Selected bond lengths (pm) of **12**: Cu1–O1 196.81(12), Cu1–O6 243.54(15), Cu1–N1 201.15(15). Symmetry code of **11**: 1−x, 2−y, 1−z. Symmetry code of **12**: 1−x, 1−y, −z.

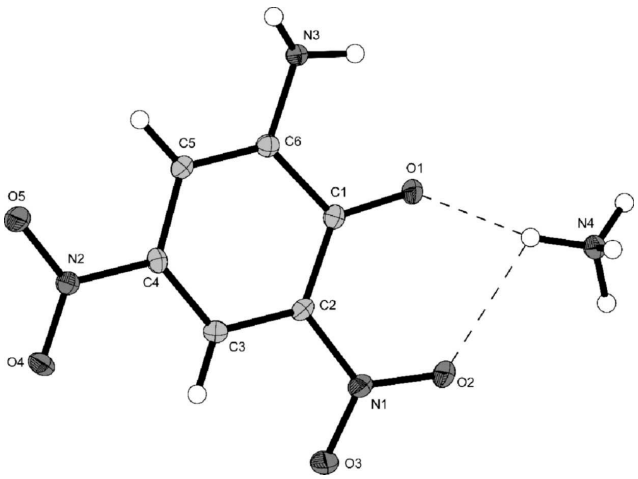

Figure 8. Molecular structure of **14**. Selected bond lengths (pm): C1–O1 126.97(17), C2–N1 144.30(18), N1–O2 123.06(17), N1–O3 123.36(17), C4–N2 143.23(18), N2–O4 123.41(15), N2–O5 124.85(16), C6–N3 139.77(18).

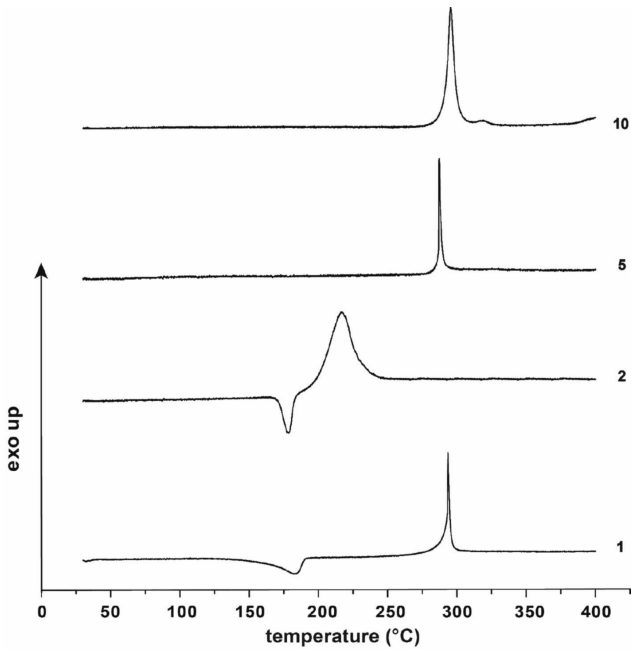

Figure 9. DTA plots of compounds **1**, **2**, **5**, and **10**.

exothermic decomposition temperatures, except the one of **13**, are all above 200 °C. Furthermore, the alkali, alkaline earth and zinc(II) picramates are even close to 300 °C, which makes those compounds to interesting energetic compounds for high-temperature applications.

The water containing compounds **3**, **7**, **8**, and **11** also show endothermic events between 79 and 223 °C, which can be matched to the loss of water. Interestingly, for the other hydrates (**4**, **9**, and **12**) no loss of water can be detected in the DTA measurements, indicating a too low sensibility of the device for minor endothermic events. Similar to picramic acid (**2**), the ammonium salt shows an endothermic event at 182 °C, that can be assigned to a melting, which was also observed during melting-point measurements. In the case of NH_4(PAM), it is directly followed by an exothermic decomposition at 209 °C (Figure S7). The relatively low thermal stability of silver picramate (**13**), is in accordance with observations made before, describing the constant decomposition starting above 120 °C [16].

Due to the difficulties in detecting the loss of water in some compounds and to further investigate the occurring endothermic events, thermogravimetric analyses (TGA) were performed. In the TGA measurements, it was heated with a heating rate of $\beta = 5\,^{\circ}\mathrm{C\,min^{-1}}$ from 30 °C to 400 °C.

In sodium picramate (**1**) the loss of 7.5 wt% can be clearly seen around 174 °C, which perfectly fits the mass of one crystal water molecule. The temperature is in accordance with the endothermic signal occurring in the DTA measurement. The same can be observed for compound **3** with a mass loss of 11 wt% at 105 °C conforming to the presence of a sesquihydrate. Due to the absence of crystal water molecules in **6** and **15**, loss of mass only can be seen at the corresponding decomposition points of the compounds (Figure 10). Similar trends can be observed for all other picramates (Figure S8–10). Special cases can be ob-

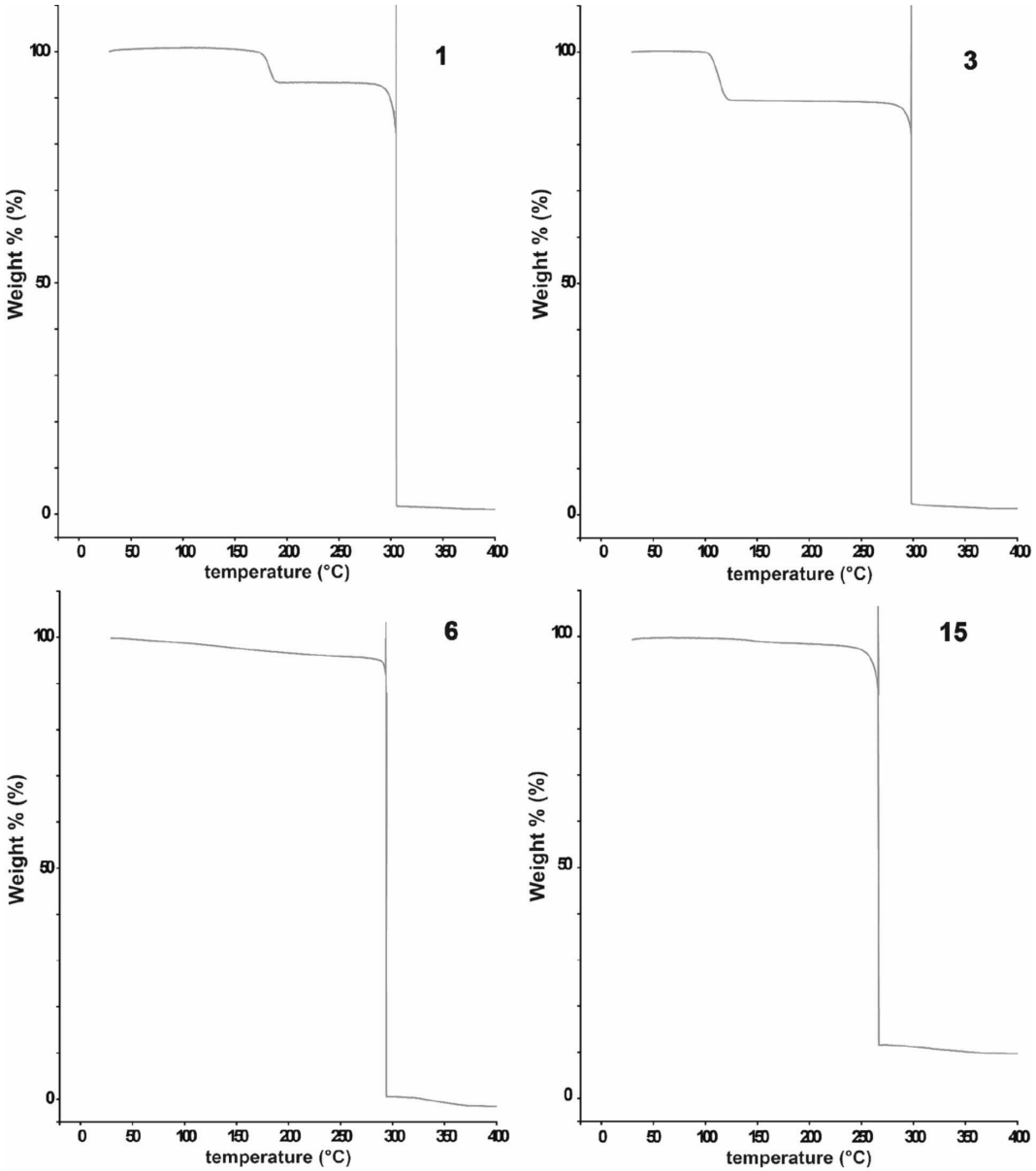

Figure 10. TGA plot of compounds **1**, **3**, **6**, and **15**.

served in substances **4** and **10**, whose compositions were verified by EA, IR, and thermal measurements. Usually, potassium salts are present as anhydrates whereas barium compounds often exist as hydrates. Therefore, both are rare examples in literature.

K(PAM)·H_2O (**4**) which shows no endothermic event during DTA measurements (Figure S5) clearly shows the loss of water till 90 °C in the TGA. When drying 4 for 24 h at 100 °C, an anhydrous substance is obtained, which immediately begins to absorb water under ambient conditions.

3.3.2 Sensitivities and Energetic Properties

Except for **10b**, all compounds were tested towards their sensitivities against impact, friction as well as electrostatic discharge (Table 1). Lead picramate (**15**) is by far the most sensitive salt of all, with values of a primary explosive ($<$1 J, 16 N). Comparing the friction sensitives, the other picramates can be classified as insensitive ($>$360 N) according to the UN Recommendations on the Transport of Dangerous Goods. The only exceptions are **6** and **13** with sensitivities of 360 N (less sensitive).

In case of impact sensitivity only compounds **2**, **3**, **7**, **11**, and **13** are ranked as insensitive, whereas **9** and **10** are less

Table 1. Thermal stability measurements by DTA[a] as well as sensitivities towards impact, friction, and ESD of **1–15**.[b]

	T_{exo}[c] (°C)	IS[d] (J)	FS[e] (N)	ESD[f] (mJ)
Na(PAM)·H_2O (**1**)	292	20	>360	>1500
HPAM (**2**)	217	>40	>360	840
Li(PAM)·1.5 H_2O (**3**)	295	>40	>360	1080
K(PAM)·H_2O (**4**)	295	10	>360	960
Rb(PAM) (**5**)	286	9	>360	540
Cs(PAM) (**6**)	287	10	360	450
$Mg(PAM)_2$·5 H_2O (**7**)	275	>40	>360	630
$Ca(PAM)_2$·2 H_2O (**8**)	300	10	>360	740
$Sr(PAM)_2$·1.5 H_2O (**9**)	288	40	>360	227
$Ba(PAM)_2$ (**10**)	291	40	>360	840
$Zn(PAM)_2$·2 H_2O (**11**)	293	>40	>360	250
$Cu(PAM)_2$·2 H_2O (**12**)	252	30	>360	270
Ag(PAM) (**13**)	156	>40	360	480
NH_4(PAM) (**14**)	209	20	>360	740
$Pb(PAM)_2$ (**15**)	259	<1	16	0.33

[a] Onset temperatures at a heating rate of 5 °C min^{-s1}. [b] Determined at a grain size <100 µm. [c] Exothermic peak, which indicates decomposition. [d] Impact sensitivity according to the BAM drop hammer (method 1 of 6). [e] Friction sensitivity according to the BAM friction tester (method 1 of 6). [f] Electrostatic discharge sensitivity (OZM ESD tester); impact: insensitive >40 J, less sensitive ≥35 J, sensitive ≥4 J, and very sensitive ≤3 J; friction: insensitive >360 N, less sensitive = 360 N, sensitive <360 N and >80 N, very sensitive ≤80 N, and extremely sensitive ≤10 N. According to the UN Recommendations on the Transport of Dangerous Goods.

sensitive. All other compounds are in the range between 9 J (**5**) and 30 J (**12**) and are therefore sensitive. The observed sensitivity of picramic acid (34 J) could not be verified in our tests. The stark contrast of the lead salt compared to all other investigated salts cannot really be explained in detail yet.

Hot needle (HN) and hot plate (HP) tests of compounds **10** and **15** prove the energetic character of the water-free picramates salts (Table 2).

Whereas barium picramate shows deflagrations in both setups (Figure 11), slight confinement of $Pb(PAM)_2$ is already leading to detonations (Figure 12).

For a better classification with already used explosives, important detonation parameters of **2** and **14** were calculated using the EXPLO5 code [25]. It can be seen that **14** is comparable to TNT with values close to it (Table 3).

As seen in Figure S11, only sodium and lithium compounds **1** and **3** could be used as potential flame colorants. Especially lithium picramate is producing an intensive red flame. All other salts show very little to no coloring, which can be explained by their low solubility.

Table 2. Hot needle and hot plate tests of **10** and **15**.

	HN[a]	HP[a]
$Ba(PAM)_2$ (**10**)	def.	def.
$Pb(PAM)_2$ (**15**)	det.	def.

[a] def.: deflagration; det.: detonation.

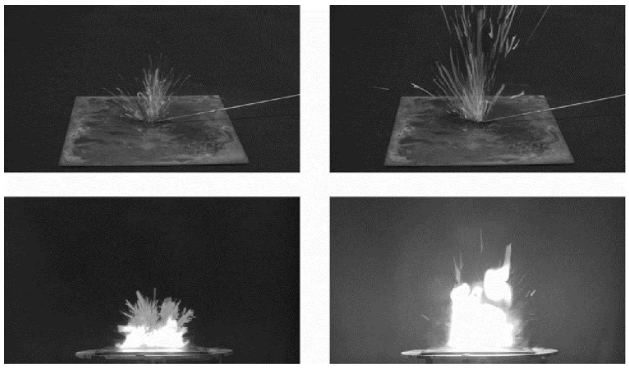

Figure 11. Hot needle (top) and hot plate (bottom) tests of compound **10**.

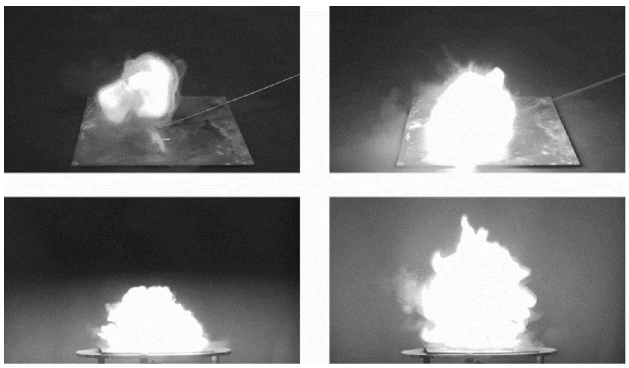

Figure 12. Hot needle (top) and hot plate (bottom) tests of compound **15**.

Table 3. EXPLO5 6.05.02 values of **2** and **14** compared to TNT.

	H(PAM) (**2**)	NH_4(PAM) (**14**)	TNT
ρ[a] [g cm^{-3}]	1.69	1.64	1.65
Ω_{CO2}[b] [%]	−76.33	−81.42	−73.96
$\triangle_f H^{o}$[c] [kJ mol^{-1}]	−1299	−1267	−261
$\triangle_f U^{o}$[d] [kJ kg^{-1}]	−1202	−1146	−171
$-\triangle_{ex} H^{o}$[e] [kJ kg^{-1}]	−3362	−3346	−4427
T_{det} [K]	2555	2423	3222
P_{CJ}[f] [GPa]	1.63	1.68	1.94
V_{det}[g] [m s^{-1}]	6546	6780	6824
V_0[h] [L kg^{-1}]	644	729	633

[a] Measured X-ray densities converted to RT. [b] Oxygen balance (Ω = (xO−2yC−1/2zH)M/1600). [c] Calculated enthalpy of formation at 298.15 K. [d] Calculated energy of formation at 298.15 K. [e] Heat of explosion. [f] Detonation pressure. [g] Detonation velocity. [h] Volume of detonation gases (assuming only gaseous products).

4 Conclusion

In this work, 14 salts of picramic acid were prepared with simple one-step acid-base reactions whereupon 11 of them were characterized by low-temperature X-ray diffraction. All intensively colored compounds (mostly red) are easily accessible by the reaction of picramic acid with the corresponding bases in hot water/ethanol and were obtained with good yields. Surprisingly, all of the investigated compounds are far less sensitive than lead(II) picramate. The calculation of the ammonium salt showed that its performance is in the range of TNT while possessing a higher decomposition temperature. Most of the metal salts show very high thermal stabilities of up to 300 °C. Especially the water-free barium picramate could be of future interest, due to its low solubility, high stability and energetic performance.

Acknowledgements

For financial support of this work by Ludwig Maximilian University (LMU), the Office of Naval Research (ONR) under grant no. ONR N00014-19-1-2078 and the Strategic Environmental Research and Development Program (SERDP) under contract no. W912HQ19 C0033 are gratefully acknowledged. The authors would like to thank Mr. Othmar Janowitz for the inspiration to investigate this topic and Dr. Peter Mayer for helping with X-ray crystal structure analysis. In addition, the authors would like to thank Mr. Moritz Kofen and Mr. Michael Gruhne for their great contribution to this work.

References

[1] J. P. Agrawal, *High Energy Materials: Propellants, Explosives and Pyrotechnics*, 1st ed., Wiley-VCH, Weinheim, **2010**.
[2] T. M. Klapötke, *Chemistry of High-Energy Materials*, 5th ed., Walter De Gruyter, Berlin, Boston, **2019**.
[3] T. M. Klapötke, *Energetic Materials Encyclopedia*, 1st ed., Walter De Gruyter, Berlin, Boston, **2018**.
[4] E. C. Johnson, E. J. Bukowski, J. J. Sabatini, R. C. Sausa, E. F. C. Byrd, M. A. Garner, D. E. Chavez, Bis(1,2,4-oxadiazolyl) Furoxan: A Promising Melt-Castable Eutectic Material of Low Sensitivity, *ChemPlusChem* **2019**, *84*, 319–322.
[5] L. L. Fershtat, N. N. Makhova, 1,2,5-Oxadiazole-Based High-Energy-Density Materials: Synthesis and Performance, *ChemPlusChem* **2020**, *85*, 13—42, doi: 10.1002/cplu.201900542.
[6] J. Zhang, Q. Zhang, T. T. Vo, D. A. Parrish, J. M. Shreeve, Energetic Salts with π-Stacking and Hydrogen-Bonding Interactions Lead the Way to Future Energetic Materials, *J. Am. Chem. Soc.* **2015**, *137*, 1697–1704.
[7] J. P. Agrawal, R. D. Hodgson, *Organic Chemistry of Explosives*, 1st ed., Wiley-VCH, Weinheim **2006**.
[8] H. Sprengel, *The Discovery of Picric Acid (Melinite, Lyddite) „As a Powerful Explosive" and of Cumulative Detonation with its Bearing on wet Gun Cotton*, 2nd ed., Eyre & Spottiswoode, London, **1903**.
[9] R. Matyáš, J. Pachman, *Primary Explosives*, 1st ed., Springer, Berlin, Heidelberg, **2013**.
[10] J. Köhler, R. Meyer, A. Homburg, *Explosivstoffe*, 10th ed., Wiley-VCH, Weinheim, **2008**.
[11] M. Nicoletti, C. Frezza, L. Tomassini, M. Serafini, A. Bianco, Detection of picramic acid and picramates in henné products by NMR Spectroscopy, *Nat. Prod. Res.* **2019**, *33*, 2073–2078.
[12] L. C. Becker, W. F. Bergfeld, D. V. Belsito, C. D. Klaassen, J. G. Jr Marks, R. C. Shank, T. J. Slaga, P. W. Snyder, F. A. Andersen, Amended Safety assessment of Sodium Picramate and Picramic Acid, *Int. J. Toxicol.* **2009**, *28*, 205–216.
[13] Z. Yang, Y. Liu, D. Liu, L. Yan, J. Chen, Synthesis and characterization of spherical 2-diazo-4,6-dinitrophenol (DDNP), *J. Hazard. Mat.* **2010**, *177*, 938–943.
[14] B. Glowiak, Thermochemical interpretation of explosive properties. I. Nitro derivatives of phenols, *Chem. Stosowana* **1961**, *5*, 575–598.
[15] S. P. Agrawal, J. P. Agrawal, Chemistry of metal picramates. I. Picramates of iron, cobalt, and nickel, *Indian J. Chem.* **1969**, *7*, 1264–1267.
[16] S. P. Agrawal, J. P. Agrawal, Chemistry of Metal Picramates – Part II (Copper and Silver), *Def. Sci. J.* **1970**, *20*, 237–248.
[17] S. P. Agrawal, B. D. Agrawal, Chemistry of zinc, cadmium, and mercury picramates, *Indian J. Chem.* **1972**, *10*, 1106–1107.
[18] R. S. Srivastava, S. P. Agrawal, H. N. Bhargava, Chemistry of Titanium, Zirconium and Thorium Picramates, *Propellants Explos. Pyrotech.* **1976**, *1*, 101–103.
[19] S. Srivastava, S. P. Agrawal, H. N. Bhargava, Synthesis, Characterization and Explosive Properties of Picramates of Palladium and Uranium, *Kogyo Kayaku* **1979**, *40*, 38–42.
[20] S. R. Yoganarasimhan, G. O. Reddy, S. Achar, Mass spectral and thermal studies on explosion of lead salts of picramic acid and 2,4-dinitrophenol, *J. Energ. Mater.* **1992**, *10*, 151–171.
[21] N. Orbovic, A. C. Luco, M. Bozovic, Production of Exploding Materials for Electro Explosive Devices, *Propellants Explos. Pyrotech.* **2008**, *33*, 271–278.
[22] L. Molard, J. Vaganay, Manufacture of picramic acid and of sodium picramate, *Meml. Poudres* **1957**, *39*, 123–136.
[23] H. Adolf, A. L. Rheingold, M. B. Allen, CCDC 1215579 **1996**.
[24] M. A. Menelaou, N. H. Fischer, F. R. Fronczek, CCDC 125117 **1999**.
[25] M. Sućeska, EXPLO5 Version 6.05.02, Zagreb, **2018**.

Manuscript received: December 3, 2019
Revised manuscript received: February 3, 2020
Version of record online: April 3, 2020